Insect Biochemistry and Molecular Biology 79 (2016) 73–86

Contents lists available at ScienceDirect

Insect Biochemistry and Molecular Biology

journal homepage: www.elsevier.com/locate/ibmb

The steroid hormone 20-hydroxyecdysone promotes switching from autophagy to apoptosis by increasing intracellular calcium levels

Yong-Bo Li, Xiang-Ru Li, Ting Yang, Jin-Xing Wang, Xiao-Fan Zhao*

Shandong Provincial Key Laboratory of Animal Cells and Developmental Biology, School of Life Sciences, Shandong University, Jinan, Shandong 250100, China

ARTICLE INFO

Article history:
Received 20 June 2016
Received in revised form
19 October 2016
Accepted 20 October 2016
Available online 21 October 2016

Keywords:
Steroid hormone
20-Hydroxyecdysone
Calcium
Autophagy
Apoptosis

ABSTRACT

Autophagy regulates cell survival (or cell death in several cases), whereas apoptosis regulates cell death. However, the relationship between autophagy and apoptosis and the regulative mechanism is unclear. We report that steroid hormone 20-hydroxyecdysone (20E) promotes switching from autophagy to apoptosis by increasing intracellular calcium levels in the midgut of the lepidopteran insect *Helicoverpa armigera*. Autophagy and apoptosis sequentially occurred during midgut programmed cell death under 20E regulation, in which lower concentrations of 20E induced microtubule-associated protein 1 light chain 3—phosphatidylethanolamine (LC3—II, also known as autophagy-related gene 8, ATG8) expression and autophagy. High concentrations of 20E induced cleavage of ATG5 to NtATG5 and pro-caspase-3 to active caspase-3, which led to a switch from autophagy to apoptosis. Blocking autophagy by knockdown of *ATG5*, *ATG7*, or *ATG12*, or with the autophagy inhibitor 3-methyladenine, inhibited 20E-induced autophagy and apoptosis. Blocking apoptosis by using the apoptosis inhibitor Ac-DEVD-CHO did not prevent 20E-induced autophagy, suggesting that apoptosis relies on autophagy. *ATG5* knockdown resulted in abnormal pupation and delayed pupation time. High concentrations of 20E induced high levels of intracellular Ca^{2+}, NtATG5, and active caspase-3, which mediated the switch from autophagy to apoptosis. Blocking 20E-mediated increase of cellular Ca^{2+} caused a decrease of NtATG5 and active caspase-3 and repressed the transformation from autophagy to apoptosis, thereby promoting cell survival. 20E induces an increase in the concentration of intracellular Ca^{2+}, thereby switching autophagic cell survival to apoptotic cell death.

1. Introduction

Autophagy is a process in which cells capture and consume their own cytoplasm and organelles to survive during stress or nutrient shortage (Rabinowitz and White, 2010). The process of autophagy mainly consists of a double-membrane autophagosome and autolysosome formation, which involves two evolutionarily conserved ubiquitin-like conjugation systems, as follows: the Atg12-Atg5 (required for autophagosome membrane formation); and ATG8 (also known as microtubule-associated protein 1 light chain, LC3). LC3 can be divided by cysteine protease and then connected to phosphatidylethanolamine (PE) to form ATG8-PE/LC3-II, which is marked in the double-membrane of autophagosomes and autolysosomes as an indicator of autophagy (Burman and Ktistakis, 2010; Liang, 2010). Apoptosis is characterized by DNA fragmentation and caspase activation; therefore, caspase activity can be used to diagnose apoptosis (Baehrecke, 2005). Caspase-3 is an apoptosis executor that indicates apoptosis (Courtiade et al., 2011). The upregulation of cleaved-caspase-3 level represents apoptosis reinforcement (Torkzadeh-Mahani et al., 2012). ATG5 is cleaved by calcium-dependent proteinase calpain to produce N-terminal ATG5 (NtATG5), which inhibits autophagy and targets NtATG5 to mitochondria, thereby inducing the release of cytochrome *c* to switch autophagy to apoptosis (Pyo et al., 2005).

In addition to autophagic cell survival, autophagic death has been reported in *Drosophila* salivary glands (Berry and Baehrecke,

Abbreviations: Ac-DEVD-CHO, N-Acetyl-Asp-Glu-Val-Asp-CHO; ATG, autophagy related; DAPI, 4-6-diamidino-2-phenylindole dihydrochloride; DMSO, dimethyl sulfoxide; GFP, green fluorescent protein; FL, flunarizine dihydrochloride; HaEpi, *Helicoverpa* epidermal cell line; HE, hematoxylinandeosin; LC3, microtubule-associated protein 1 light chain 3; NtATG5, N-terminal ATG5; PYR3, pyrazole compound; RFP, red fluorescent protein; XeC, xectospongin C; 3-MA, *3-Methyladenine*; 20E, 20-hydroxyecdysone.

* Corresponding author.
E-mail address: xfzhao@sdu.edu.cn (X.-F. Zhao).

http://dx.doi.org/10.1016/j.ibmb.2016.10.004
0965-1748/

2007). Autophagy can also be converted to apoptosis under excessive interleukin-24 stimulation as the knockdown/knockout of autophagy-related genes (ATGs) reduces cell death (Bhutia et al., 2011), whereas apoptosis results in cell death (Zocchi et al., 1998). Inhibition or deficiency of apoptosis protein caspase8 results in excessive autophagy (Yu et al., 2004), and inhibition of autophagy induces apoptosis (Fang et al., 2014), thereby suggesting counteractive roles between autophagy and apoptosis. The relationship among autophagy, apoptosis, and the regulatory mechanisms are complicated and are not completely demonstrated (Tracy and Baehrecke, 2013).

Calcium mobilization and homeostasis in cells are important for a number of cellular functions (Berridge et al., 2000). Cytosolic Ca^{2+} is kept at low levels (10–100 nM), whereas extracellular Ca^{2+} is maintained at much higher levels (Clapham, 2007). In a few cell types, increasing Ca^{2+} can trigger autophagy, whereas increasing Ca^{2+} in others can activate calpain to cleave ATG in order to generate ATG5 to NtATG5, thereby inhibiting autophagy but promoting apoptosis (Friedrich, 2004; Herrero-Martin et al., 2009; Hoyer-Hansen et al., 2007; Pinter and Friedrich, 1988; Pyo et al., 2005). Ca^{2+} could be the key factor in regulating autophagy and apoptosis. However, the regulation role of Ca^{2+} in either autophagy or apoptosis is unclear.

The midgut undergoes remodeling, which involves the degradation of larval midgut and the formation of an imaginal midgut during metamorphosis in insects (Hakim et al., 2010). The degradation of the larval midgut is involved in programmed cell death (PCD); this process provides nutrients for the imaginal midgut formation in lepidoptera (Tettamanti et al., 2007).

The midgut PCD in dipteran *Drosophila* resulted from autophagic cell death but not apoptotic cell death (Denton et al., 2009). *Drosophila* midgut autophagy and apoptosis are both enhanced by steroid hormone 20E (Santhanam et al., 2014). Autophagy and apoptosis sequentially occurred in midgut PCD in lepidopteran *Bombyx* (Franzetti et al., 2012). The steroid hormone 20E promotes midgut PCD (Iga et al., 2010; Manaboon et al., 2009). 20E also promotes autophagy-related and apoptosis-related gene expression (Romanelli et al., 2014). Moreover, 20E can induce an intracellular Ca^{2+} increase to promote apoptosis in the lepidopteran insect *H. armigera* (Cai et al., 2014; Liu et al., 2014; Wang et al., 2016). Therefore, the 20E-induced midgut PCD is a good model for studying the relationship between autophagy and apoptosis.

H. armigera, a *Lepidopteran* insect that is considered a serious agricultural pest, was used as the model for these experiments. High 20E concentration induces high intracellular Ca^{2+} levels, which induces the transformation from autophagy to apoptosis. Higher Ca^{2+} levels regulate ATG5 cleavage to NtATG5 to active caspase-3 for apoptosis. Autophagy maintains cell survival whereas apoptosis results in cell death. The higher concentration of intracellular Ca^{2+} switches autophagic cell survival to apoptotic cell death under 20E induction.

2. Materials and methods

2.1. Animals and cell culture

H. armigera larva were raised on an artificial diet at 28 °C with a dark to light (10:14 h) in the laboratory. The *H. armigera* epidermal cell line (HaEpi) was cultured at 26 °C and was seeded in 4 mL of Grace's medium including 10% inactivated bovine serum without any antibiotics (Shao et al., 2008). All of the experiments were carried out at a density of 5×10^5 cells and were maintained under normal growth conditions for 96 h.

2.2. 20E treatment of HaEpi cells

The HaEpi cells were cultured with 5 μM 20E (Sigma, St Louis, MO, USA) for 1, 6, 24, 48, or 72 h or cultured with 1, 2, 5, 10 μM 20E for 24 h in Grace's medium at 27 °C. The same volume of dimethylsulfoxide (DMSO) was added as a 20E solvent control. The total proteins were extracted from cells with 40 mM Tri-HCl for Western blot assays.

2.3. Western blot

The Bradford method was used to determine the protein concentration (Bradford, 1976). Fifty micrograms of protein were separated by sodium dodecyl sulfate-polyacrylamide gel electrophoresis (SDS-PAGE) (12.5%) and then transferred onto nitrocellulose membranes. The membranes were incubated for 1 h at room temperature in blocking buffer consisting of a 10 mM Tri-buffered saline (TBS) solution and 2–5% fat-free powdered milk. The primary rabbit anti-LC3, ATG5 or Caspase-3 polyclonal antibody was added into the blocking buffer (1:100 diluted) overnight at 4 °C, and then, the secondary rabbit antibody, labeled with alkaline phosphatase, was added at a dilution of 1:10000 in blocking buffer. The Western blot signal was observed in 10 mL of a Tri-buffered saline solution combined with 45 μL of 5% p-nitro-blue tetrazolium chloride (NBT) and 35 μL of 5% 5-bromo-4-chloro-3-indolyl phosphate (BCIP) in the dark for 10 min. Quantitative analysis of Western bands was performed by Quantity One® software.

2.4. Autophagy detection

The anti-rabbit polyclonal antibody against *H. armigera* LC3 was prepared to detect LC3 by Western blot analysis. *H. armigera* full length LC3 was expressed in *Escherichia coli* by a *PET-30a* plasmid. Two-hundred micrograms of purified LC3 in 1 mL of TBS was mixed with 1 mL of complete Freund's adjuvant and injected into a rabbit subcutaneously to prepare the antibody according to the previous description (Sui et al., 2009). ATG5 antiserum was prepared by the same method. The green fluorescence protein (GFP) was fused with LC3 to produce GFP-LC3-II to indicate the development of autophagy from autophagosomes to autolysosomes by GFP laminating fluorescence at neutral pH in autophagosomes and quenching at acidic pH in autolysosomes (Tasdemir et al., 2008). A RFP-GFP-LC3-His fusion protein was overexpressed for 48 h in HaEpi cells by *pIEx-4-RFP-GFP-LC3-His* reporter plasmid to detect autophagosomes and autolysosomes. A cell-penetrating TAT peptide (TATGGCAGGAAGAAGCGGAGACAGCGACGAAGA) (Zhou et al., 2015) was fused with RFP and LC3 (His-TAT-RFP-LC3-His) and was expressed in *E. coli* by the *pET30a-TAT-RFP-LC3* plasmid. His-TAT-RFP-LC3-His was purified to detect autophagosomes in HaEpi cells. The autophagy inhibitor *3-Methyladenine* (10 μM, 3-MA, NO. 5142-23-4, Gene Operation, USA) was added or injected *as a negative control* in HaEpi cells or the midgut, respectively, to detect the expression of LC3/autophagosomes in HaEpi cells and midgut.

2.5. Immunohistochemistry

The larval midgut was isolated and then treated with 4% paraformaldehyde at 4 °C overnight and gradient-dehydrated. The prepared midgut tissues were embedded in paraffin, cut into 7-μm sections, adhered to gelatin-coated glass slides, and dried at 42 °C overnight. The slides were dewaxed, gradient-rehydrated and then digested with 20 μM proteinase K at 37 °C for 10 min. The slides were blocked in blocking buffer for 30 min at 37 °C and a rabbit anti-*H. armigera* LC3 polyclonal antibody (1: 100) or anti-human, mouse, rat Caspase-3 polyclonal antibody (pAb) (1: 300) (WL01589, Wanleibio,

Shen Yang, China) was added overnight at 4 °C. The slides were washed with phosphate buffered saline (PBS: 10 mM Tris-HCl, pH 7.5; 150 mM NaCl) three times, and then, 1 μL of a secondary antibody against goat IgG labeled with Alexa Fluor 488 (anti-rabbit-Alexa Fluor 488) was added to 10 mL of blocking buffer at 37 °C for 1 h. The nuclei were stained with 1 μg/mL DAPI (4′, 6-diamidino-2-phenylindole) (AnaSpec, Inc., San Jose, CA, USA) for 10 min at room temperature. An Olympus BX51 fluorescence microscope (Shinjuku-ku, Tokyo, Japan) was used to observe fluorescent.

2.6. Hematoxylin eosin (HE) staining

The rehydrated histologic sections were stained by hematoxylin (hematoxylin 1 g, 10 mL of ethanol, 20 g of $KAl(SO4)_2$ 200 mL of H_2O) for 10 min, washed with running water for 1 min and stained with Scott TapWater/Bluing (0.35 g of NaHCO3 and 2 g of MgSO4 dissolved PBS) for 1 min. They were then washed with hydrochloric acid ethanol differentiation medium (70% ethanol in 1% hydrochloric acid) for 20 s, stained with Scott TapWater/Bluing for 1 min, washed with 1% ammonia water for 30 s, incubated with a 0.5% eosin staining solution for 30 s, and then washed with water for 1 min. The images were observed with an Olympus BX51 fluorescence microscope.

2.7. RNA interference (RNAi) in larvae and HaEpi cells

dsRNA was synthesized using a MEGAscriptTM RNAi kit (Ambion, Austin, Texas, USA). In HaEpi cells, 500 ng of *dsRNA* of ATG5 (*dsATG5*, 499 bp) was mixed with 5 μL of QuickShuttle-enhanced transfection reagent (Beijing immunotechnologies corporation China) in 2 mL of Grace's medium, and 500 ng of *dsRNA* of GFP (*dsGFP*, 513 bp) was used as a non-specific RNAi control. Cells were cultured for 48 h after transfection with *dsATG5* or *dsGFP* in Grace's medium and 5 μM 20E was subsequently added. In larvae, 6th instar 6 h larvae were injected with 500 ng of *dsATG5* or *dsGFP* and 500 ng of 20E.

2.8. Quantitative real-time PCR (qRT-PCR)

We extracted total RNA from treated cells and midgut with TRIzol Reagent according to the manufacturers' instructions (CWbio Beijing, China). cDNA was synthesized according to the FastQuant RT Kit (TIANGEN BIOTECH Beijing, China. qRT-PCR was carried out with a Power 2 × SYBR real-time PCR pre-mixture (BioTeke Corporation Beijing, China), and a real-time thermal cycler (Bio-Rad, Hercules, CA, USA). *H. armigera β-actin* (Gene Bank number EU52707) was used for internal standardization. All analyses used data from three independent experiments by $2^{-\triangle\triangle CT}$ (Liu et al., 2011) and Student's *t*-test. The primers were listed in Table 1.

2.9. Detection of the cellular Ca^{2+} level in midgut and HaEpi cells

The midguts from three 6th instar 48, 72, 96, and 120 h larvae were dissected to examine the endogenous calcium level. Different doses of 20E (100, 200, 500, 1000 ng) were injected into the hemolymph of 6th instar 6 h larvae to examine the 20E-induced calcium level. The midgut was washed in PBS and then incubated in 1 mL of PBS with 3 μM AM ester Calcium Crimson TM dye (Invitrogen, Carlsbad, CA, USA) for 30 min at 27 °C. After being washed three times with PBS, the midgut was frozen and sectioned to 7 μm, and red fluorescence was observed by an Olympus BX51 fluorescence microscope. We used frozen sections for midgut experiments. The possibility of calcium homeostasis disruption during freezing the tissues cannot be excluded. However, a certain amount of calcium was trapped in the left tissues. This method was used as described in a previous study (Liu et al., 2015) with some improvements. HaEpi cells were treated with 20E for different times and concentrations in Grace's medium and then incubated with 3 μM AM ester Calcium CrimsonTM dye in 1 mL of DPBS (KCl 0.2 g/L, $MgCl_2$ 0.047 g/L, Na_2HPO_3 1.158 g/L, NaH_2PO_3 0.2 g/L, NaCl 8.0 g/L, H2O 1000 mL, PH7.4) for 30 min at 27 °C. After being washed with PBS three times, red fluorescent cells were observed using an Olympus BX51 fluorescence microscope. To measure the calcium levels induced by different 20E concentrations, we used separate cell samples for 20E and DMSO treatments. F and F0 showed the difference between 20E and DMSO treatments in 24 h in cell images; and this method has been reported previously (Wang et al., 2013). The intensity of calcium signal was observed and statistically analyzed. We have published a separate paper demonstrating the 20E concentration-dependent calcium increase (Wang et al., 2016).

Table 1
Primers used in the experiments.

Primer name	Sequence (**5′-3′**)
ATG5-RTF	ATGGCTAACGATAGAGAAG
ATG5-RTR	AGTTAGATGCCACGGAAG
ATG7-RTF	AAGCCAGCGTGCCTCCCTA
ATG7-RTR	CTGTCTGAATGGCGGGCGA
ATG12-RTF	CACCGTCACCAGACCAGTTAG
ATG12-RTR	TGATTTCCCACAATGAACCTTA
ATG5RNAiF	TAATACGACTCACTATAGGATGAAAAGACACTTCCTG
ATG5RNAiR	TAATACGACTCACTATAGGTTGCAATGTCTTCCTAC
ATG7RNAiF	TAATACGACTCACTATAGGGTTCAGTTATCGTGGCG
ATG7RNAiR	TAATACGACTCACTATAGGGAGTTGGGCAGTGGTCT
ATG12RNAiF	TAATACGACTCACTATAGGAAATAAATGGGTGACGAAAAGC
ATG12 RNAiR	TAATACGACTCACTATAGGCTAACTGGTCTGGTGACGGTGC
caspase-3RNAiF	TAATACGACTCACTATAGGATGTGTGTCACTATCCTG
caspase-3RNAiR	TAATACGACTCACTATAGGAAATTTCAGCAGCAGCTTTG
GFPRNAiF	GCGTAATACGACTCACTATAGGTGGTCCCAATTCTCGTGGAAC
GFPRNAiR	GCGTAATACGACTCACTATAGGCTTGAAGTTGACCTTGATGCC
ATG5exF	TACTCAGAATTCAAGATGAAAAGACAC
ATG5exR	TACTCACTCGAGTCAATGTGATTCCATCAA
LC3exF	TACTCAGGATCCATGAATTCCAATATAAAG
LC3exR	TACTCAGAGGTCATATCCATATACATTC
LC3GBDF	TACTCAGCGGCCGCAATGAATTCCAATATAAAG
LC3GBDR	TACTCACTCGAGATATCCATATACATTC
RFPF	TACTCAGAGCTCATGGCCTCCTCCGAGGACGTC
RFPR	TACTCAAGATCTGGGCGCCGGTGGAGTGGCGGCC
GFPF	TACTCAAGATCTCGATGAGCAAGGGCGAGGAAC
GFPR	TACTCAGCGGCCGCTCTTGTACAGCTCGTCCAT

2.10. Apoptosis detection

HaEpi cells were incubated with 5 μM 20E for 1, 6, 24, 48, and 72 h or with 1, 2, 5, or 10 μM 20E for 24. Anti-human, mouse, rat Caspase-3 polyclonal antibody (pAb) was used to detect the active caspase-3 band in a Western blot assay, and the addition of 10 μM Ac-DEVD-CHO (a caspase-3 activity inhibitor, NO. 30029 Biotium, Hayward, USA) repressed apoptosis. The NucView™ caspase-3 assay kit (NO. 30029 Biotium, Hayward, USA) was used to detect caspase-3 activity in HaEpi cells by immunocytochemistry according to the manufacturer's instructions. Annexin-V and Propidium Iodide (PI) were used to detect apoptosis according to Annexin V-FITC Apoptosis Detection kit (GK3603, GENVIEW, USA).

2.11. Cell death detection

Trypan blue (4%, 4 g of trypan blue powder diluted in 100 mL of H_2O) was used to identify dead cells. HaEpi cells were treated with 20E for different times and concentrations. Two μL of 4% trypan blue was mixed with 200 μL of PBS and incubated with cells for 3 min. The cells were washed with PBS three times and observed by differential interference microscopy.

2.12. GenBank accession numbers of H. armigera genes

ATG5, KT895433.1, the accession number will be released by GenBank after the paper is published; *LC3*, JQ739159.1; *caspase-3*, HQ328962.1.

3. Results

3.1. Autophagy and apoptosis sequentially occurred in the larval midgut during larval development

The expression profiles of ATG5, LC3, and caspase-3 in the midgut were analyzed by Western blot analysis to show the occurrence of autophagy and apoptosis. ATG5 appeared as full-length ATG5 and cleaved ATG5 (NtATG5) during the larval growth stages from the 5th instar feeding (5F) to the 6th instar feeding (6–48 h). However, NtATG5 decreased during the molting (5M) and metamorphic stages from 6–72 h to 6–120 h and reappeared at the pupation stage (Fig. 1A and a). Correlating with the decrease of NtATG5, ATG5 increased from 6–72 h to 6–120 h but decreased at the pupation stage, and LC3-II appeared at 6–72 and 6–96 h but decreased at 6–120 h and the pupal stages during metamorphosis (Fig. 1B and b). Cleaved-caspase-3 emerged at 6–120 h and the pupal stages, and the total expression levels of Pro-caspase-3 were

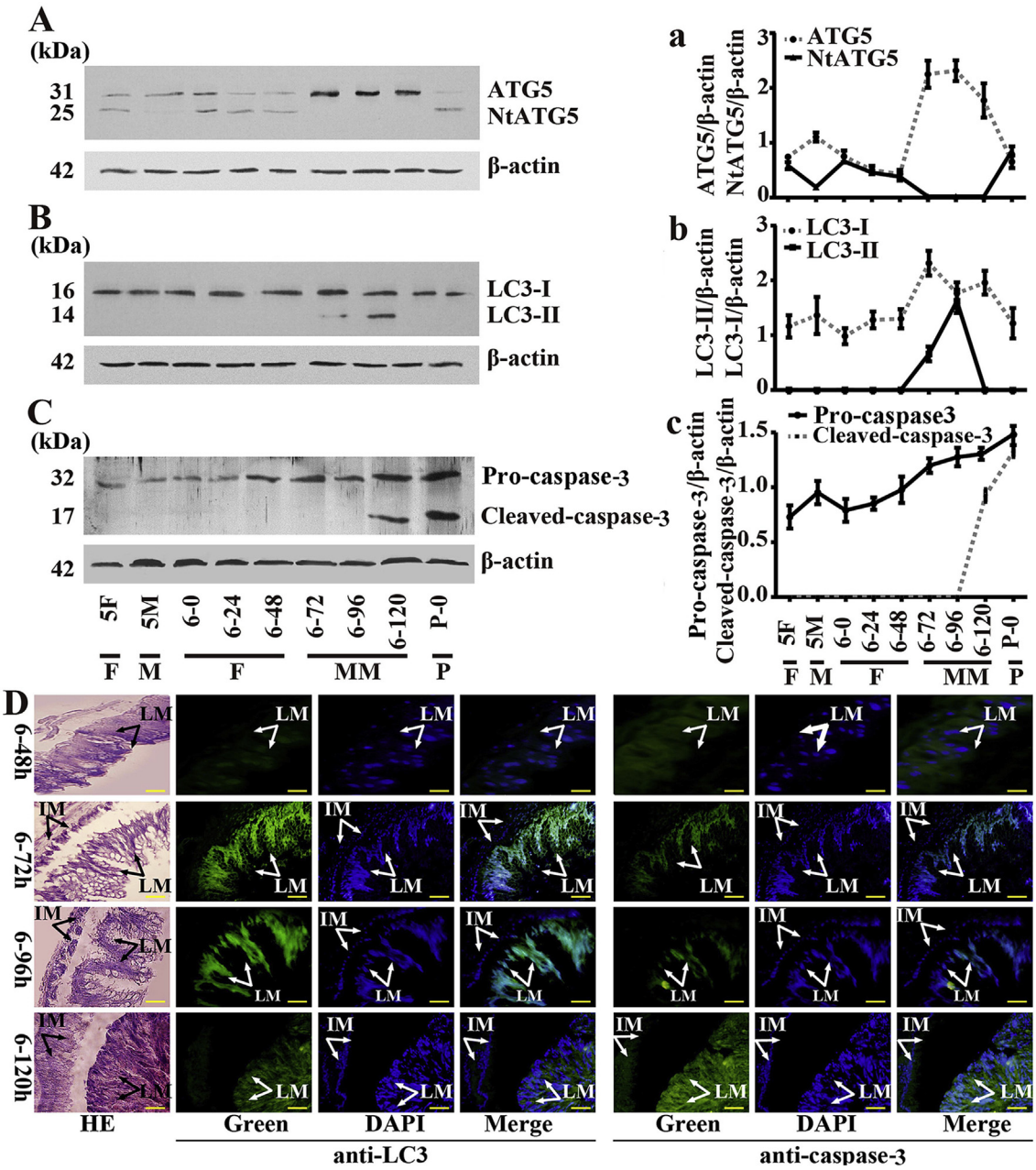

Fig. 1. The variation of the expression profiles of ATG5, LC3 and caspase-3 in the larval midgut. (A), (B) and (C) Western blot analysis of ATG5 (full length) and NtATG5 (N terminal ATG5), LC3-I and LC3-II, and Pro-caspase-3 and Cleaved caspase-3, respectively. 5F: fifth instar feeding larvae; 5M: fifth instar molting larvae; 6-0 h, 6–24 h, 6–48 h, 6–72 h, 6–96 h, and 6–120 h indicate the development hours of sixth instar larvae; p-0 h: 0 h pupation. β-actin was used as an internal reference. **(a), (b) and (c)** Quantitative analysis of (A), (B) and (C). **(D)** Localization of LC3 and Caspase-3 in the midgut. LM: larval midgut; IM: imaginal midgut; HE staining showed the morphology of the midgut; green fluorescence indicated LC3 and Caspase-3 stained by polyclonal anti-*Helicverpa*-LC3 and anti-*Helicverpa*-caspase-3 serum, respectively, and the Alexa 488-labeled secondary antibody. Blue fluorescence indicated nuclei stained by DAPI. The merge indicated the fusion of green and blue fluorescence. All experiments were performed in triplicate, and bars represented the mean ± S. D. The yellow bars represented 10 μm. (For interpretation of the references to colour in this figure legend, the reader is referred to the web version of this article.)

increased following the decrease of LC3-II (Fig. 1C and c). Immunohistochemistry showed that LC3 was mainly localized in the larval midgut at 6–72 h and 6–96 h. However, clear autophagic dots were not observed because the tissue section showed overlapping cells. Caspase-3 was also localized in the larval midgut, with an increase in caspase-3 signal at 6–120 h (Fig. 1D). These results suggest that autophagy and apoptosis occur in the larval midgut during midgut PCD, whereas autophagy occurs before apoptosis.

3.2. 20E regulated autophagy transforming to apoptosis based on time or concentration

After induction with 5 μM 20E, ATG5 and LC3-II gradually increased over 24 h, thereby indicating the occurrence of autophagy. Between 48 and 72 h, ATG5 was cleaved to NtATG5, and cleaved-caspase-3 increased; these phenomena are consistent with the occurrence of apoptosis (Fig. 2A and a). The activity of caspase-3 was further detected by a caspase-3 activity assay, in which the cells were treated with 20E, as described in the Methods. The caspase-3 assay kit worked well in HaEpi cells (Zhao et al., 2016). Green fluorescence indicated the presence of caspase-3 activity at 72 h after 20E induction, whereas Trypan blue staining indicated cell death (Fig. 2B and b). These data suggest that 5 μM 20E initiates autophagy in a short period of time, whereas the transformation of autophagy to apoptosis occurs in 72 h.

The effect of the 20E concentration on switching autophagy to apoptosis was further investigated in HaEpi cells after 24 h to examine the effect of 20E concentration on the transformation of autophagy to apoptosis. 20E (1 μM) induced neither LC3-II nor NtATG5 and cleaved-caspase-3 formation in 24 h, indicating that neither autophagy nor apoptosis occurred in response to the treatment. 20E (2 μM–5 μM) induced the increased expression of ATG5 and LC3-II but did not induce NtATG5 and cleaved-caspase-3 formation, indicating that autophagy and not apoptosis occurred in the cells in 24 h. 20E (10 μM) induced a decrease of ATG5 and LC3-II, whereas a NtATG5 and cleaved-caspase-3 increased, indicating that autophagy decreased, and apoptosis occurred in 24 h by 10 μM 20E treatment (Fig. 2C and 2c). In correlation with the transformation of the protein forms, active caspase-3 was detected in the cells by a caspase-3 activity assay. The green dots confirmed caspase-3 activity, in which the cells were treated with 10 μM 20E in 24 h, and Trypan blue staining indicated cell death (Fig. 2D and 2d). These data suggest that 20E induces autophagy at a relatively low concentration, whereas 20E induces apoptosis at a higher concentration in 24 h.

3.3. 20E induced autophagosome and autolysosome formation

Red and green fluorescence proteins were fused with LC3 (RFP-GFP-LC3) and were overexpressed in HaEpi cells to examine 20E-induced autophagosome and autolysosome formation. After 5 μM 20E induction for 1 h, RFP-GFP-LC3 appeared as uniform red and green fluorescence in cells. After 6 h, RFP-GFP-LC3 appeared as autophagic vacuoles exhibiting both RFP and GFP fluorescence, indicating the formation of an autophagosome. The green fluorescence was quenched in 24 h, indicating the formation of an autolysosome; the acidity of the autolysosome quenched the GFP fluorescence. However, the autophagic vacuoles disappeared in 72 h, indicating that autophagy did not continuously occur. For the disappearance of autophagic vacuoles, RFP-GFP-LC3 protein only diffused in the cytoplasm, which presented green and red fluorescence. DMSO, which is the hormone solvent control, did not induce autophagosome formation at all times (Fig. 3). These data confirm that 20E induces autophagosome and autolysosome formation. However, autolysosome was not consistently present in 72 h.

3.4. Autophagic proteins are necessary for apoptosis following the stimulation with 20E

ATGs knockdown, autophagy inhibitor *3-methyladenine* (3-MA), and a caspase-3 inhibitor Ac-DEVD-CHO (Ac-DEVD) were used to study the relationship between 20E-induced autophagy and apoptosis. Knockdown of *ATG5* by RNA interference or treatment with 3-MA decreased the LC3-II level, whereas Ac-DEVD-CHO did not decrease the LC3-II level, thereby suggesting that autophagy relies on ATG5 (Fig. 4A). However, *ATG5* knockdown or treatment with 3-MA decreased the cleaved-caspasae3 level (Fig. 4B), thereby suggesting that apoptosis also relies on ATG5.

A cell-penetrating peptide (TAT) (Zhou et al., 2015) fused RFP-LC3 (His-TAT-RFP-LC3-His) and caspase-3 activity were observed to confirm the preceding hypothesis. Knockdown of *ATG5* or blocking autophagy using 3-MA repressed the formation of autophagosomes, but the caspase-3 inhibitor Ac-DEVD-CHO did not repress the formation of autophagosomes (Fig. 4C). Regarding the blocking of autophagy, knockdown of *ATG5* or blocking autophagy by 3-MA repressed the activity of caspase-3, as indicated by green dots. Cell death was also inhibited by the knockdown of *ATG5* or blocking autophagy using 3-MA as indicated by Trypan blue staining (Fig. 4D), thereby suggesting that autophagic protein ATG5 is necessary for apoptosis after 20E stimulation.

ATG5, *ATG7*, or *ATG12* was also knocked down to further confirm that autophagic proteins are essential to apoptosis. *ATG5*, *ATG7*, or *ATG12* was significantly knocked down in 24 and 72 h (Fig. 5A and B). The LC3-II level presented a significant decrease compared to the *dsGFP* control after knockdown of *ATG5*, *7*, or *12* (Fig. 5C). The cleaved-caspase-3 level also decreased with decreasing LC3-II (Fig. 5D). In addition, the number of pyknotic cell nucleus drastically declined after knockdown of *ATG5*, *ATG7*, or *ATG12* (Fig. 5E). Flow cytometry analysis also showed that the rate of apoptotic cells significantly decreased after knockdown of *ATG5*, *ATG7*, or *ATG12* (Fig. 5F and G). These results confirm that autophagic proteins are necessary for apoptosis following 20E stimulation.

3.5. Knockdown of ATG5 in larvae repressed autophagy, apoptosis, and midgut PCD

ATG5 was knocked down in larvae to examine the function of ATG5 20E-induced pupation and midgut PCD. *ATG5* knockdown resulted in abnormal pupation (Fig. 6A) and delayed midgut PCD (Fig. 6B). Ten percent of larvae formed abnormal pupae after *ATG5* knockdown (Fig. 6C). In addition, the pupation time including normal and abnormal pupation was delayed for 24 h after *ATG5* knockdown (Fig. 6D). The Western blot assay showed that *ATG5*-knockdown decreased 20E-induced LC3-II and cleaved-caspase-3 levels in the 6th instar 96 h after larval midgut (Fig. 6E and e). These results suggest that 20E via ATG5 promotes autophagy and apoptosis for larval midgut PCD.

3.6. Calcium determined the 20E-induced formation of NtATG5, cleaved-caspase-3, and apoptosis

Intracellular Ca^{2+} concentration was analyzed to determine the mechanism of the 20E-induced transformation of autophagy to apoptosis. NtATG5 is cleaved by a calcium-activated protease called calpain, which inhibits autophagy and targets the mitochondria to induce the release of cytochrome *c* and activate caspases (Shi et al., 2013). HaEpi cells were incubated in calcium-free PBS. Different concentrations of Ca^{2+} plus equal diluted DMSO were added as the

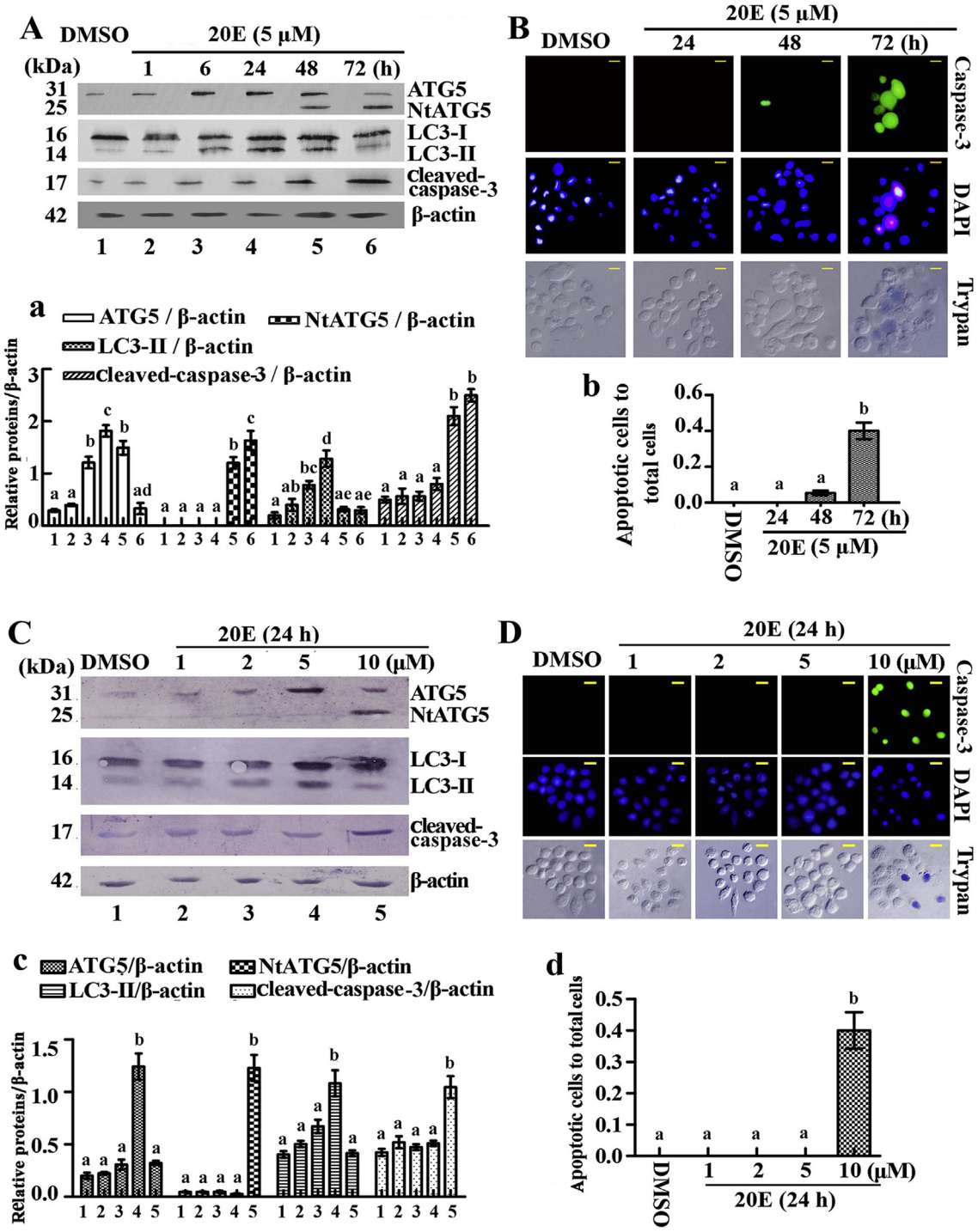

Fig. 2. 20E-regulated autophagy transformation to apoptosis based on time or the concentration of 20E induction in HaEpi cells. (A) Western blot assay for the expression of ATG5, LC3-I, LC3-II and Cleaved-caspase-3 after 20E (5 μM) induction for different durations, with *H. armigera* β-actin as the control. **(a)** Statistical analysis of A. **(B)** Examination of apoptosis. 20E 5 μM; DMSO was a solvent control; Caspase-3 (green fluorescence) was detected using a NucView™ caspase-3 activity assay kit; Trypan blue-stained cells indicated dead cells (light blue color); DAPI stained the nucleus (blue fluorescence); other treatments were the same as in A. **(b)** Statistical analysis of B. **(C)** Western blot assay for ATG5, NtATG5, LC3-I, LC3-II and Cleaved-caspase-3 after 20E (1, 2, 5, 10 μM) induction for 24 h with β-actin as the control. **(c)** Statistical analysis of C. **(D)** Examination of apoptosis by the same 20E treatments as in C. The graphical representation was the same as in B. **(d)** Statistical analysis of D. All experiments were performed in triplicate, and statistical analysis was conducted using ANOVA. Bars represented the mean ± S. D, and different lowercase letters indicated significant differences ($p < 0.05$). The yellow bars represented 20 μm. (For interpretation of the references to colour in this figure legend, the reader is referred to the web version of this article.)

control. Different concentrations of Ca^{2+} plus 5 μM 20E were added as the experimental group. ATG5 was gradually converted to NtATG5 in the experimental group. Meanwhile, the LC3-II level decreased, and the cleaved-caspase-3 level increased (Fig. 7A and a). In contrast, when Ca^{2+} channel inhibitors were added, ATG5 was not cleaved by 20E plus Ca^{2+} treatment. The inhibitors included dihydrochloride (FL), a T-type voltage-gated calcium channel inhibitor (Terland and Flatmark, 1999); pyrazole compound (PYR3), a

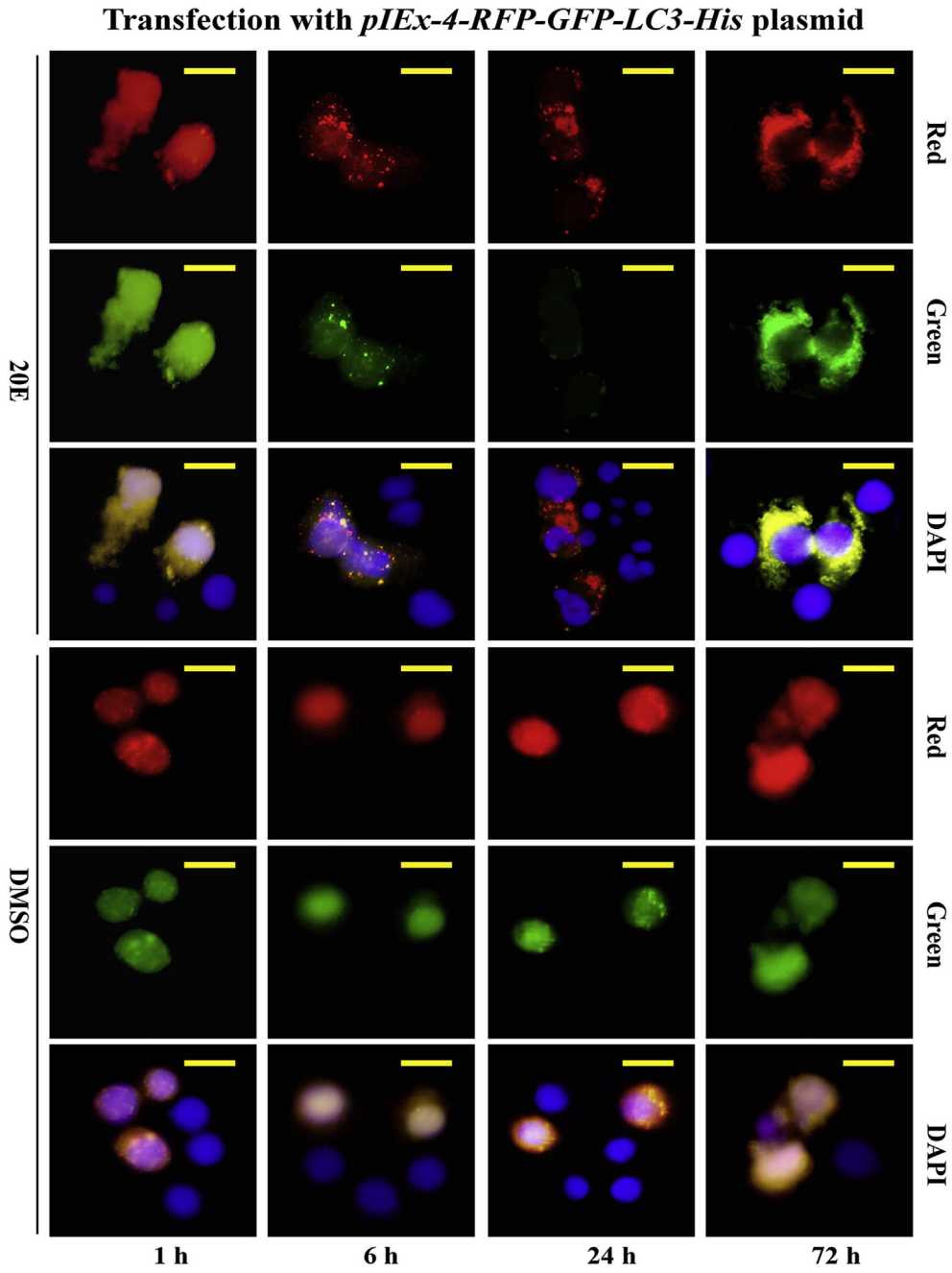

Fig. 3. 20E induced autophagosome formation. Green: indicating green fluorescence. Red: indicating red fluorescence. DAPI: indicating nuclei stained as blue fluorescence. DMSO: solvent control. 20E: experiment treatment (5 μM). The yellow bars represented 20 μm. (For interpretation of the references to colour in this figure legend, the reader is referred to the web version of this article.)

transient receptor potential calcium channel inhibitor, (Kiyonaka et al., 2009); and XeC, an inositol 1,4,5-triphosphate (IP3) receptor inhibitor (De Smet et al., 1999). LC3-II significantly increased, and cleaved-caspase-3 decreased compared with the treatment with 20E plus Ca^{2+} (Fig. 7B and b). The data shows that the cleavage of ATG5 and caspase-3 depends on the increase of the calcium concentration after 20E induction.

The Ca^{2+}-mediated transformation between autophagy and apoptosis was further examined in HaEpi cells to confirm the above-mentioned hypotheses. The apoptosis signal of caspase-3 activity was relatively stronger in the cells treated with 20E plus Ca^{2+} than other treatments, including DMSO, 20E alone, or 20E plus Ca^{2+} with calcium channel inhibitors (Fig. 7C and c), thereby indicating that calcium promoted 20E-mediated apoptosis. In contrast, red autophagic vacuoles indicated by TAT-RFP-LC3 were fewer in the cells treated with 20E plus Ca^{2+} compared with other treatments, including DMSO, 20E alone, or 20E plus Ca^{2+} with calcium channel inhibitors (Fig. 7D and d), thereby indicating that calcium repressed 20E-induced autophagy. These data suggest that Ca^{2+} regulated the transformation of 20E-induced autophagy to apoptosis.

3.7. 20E increased intracellular Ca^{2+} level in a dose-dependent manner

The Ca^{2+} level was examined in the larval midgut at 6–48, 6–72, 6–96, and 6–120 h to demonstrate the increase of the Ca^{2+}

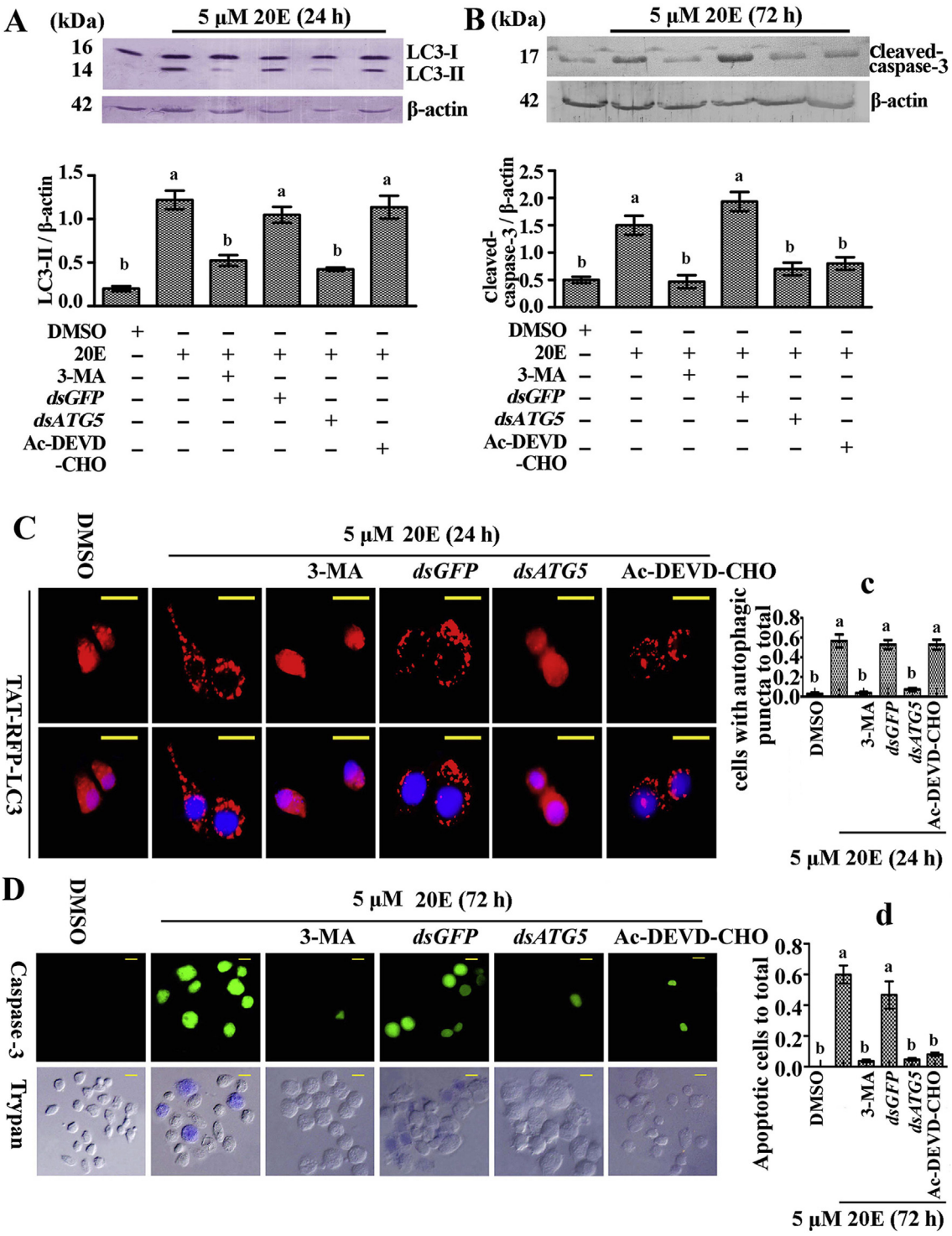

Fig. 4. Autophagic proteins are necessary for apoptosis. **(A)** Statistical analysis of the expression of LC3-II based on a Western blot assay. β-actin as the loading control and *dsGFP* (500 ng for 48 h) as the negative control of *dsATG5* and *dsATG5* (500 ng for 48 h). 3-MA (10 μM), Ac-DEVD-CHO (10 μM), 20E (5 μM for 24 h), DMSO as the solvent control of 20E. **(B)** Statistical analysis of the expression of Cleaved-caspase-3 using the same treatments as in A, except the 20E (5 μM) induction was for 72 h **(C)** and **(D)** Examination of autophagy and apoptosis by the addition of purified TAT-RFP-LC3 protein from *E. coli* Rosetta host cells (2 μg in 2 ml Grace's medium) and active caspase-3, respectively, under 20E induction (5 μM for 24 h) with the same treatments as in B. (c) and (d) Quantification of cells with autophagic puncta to total and apoptotic cells to total. All of the experiments were performed in triplicate, and statistical analysis was conducted using ANOVA. Bars represented the mean ± S. D. and different lowercase letters indicated significant differences ($p < 0.05$). The yellow bars represented 20 μm. (For interpretation of the references to colour in this figure legend, the reader is referred to the web version of this article.)

level during midgut PCD. Red fluorescence from AM ester Calcium Crimson TM dye increased along with the larval development from the 6th instar 48 h to the 6th instar 120 h along with the midgut PCD (Fig. 8A). Different concentrations of 20E were injected into the hemolymph of the 6th instar 6 h larvae to verify the 20E induction of Ca^{2+} increase in the midgut in 24 h. Red fluorescence indicated that the Ca^{2+} level increased along with the increased 20E concentration (Fig. 8B). These data suggest that 20E induces calcium

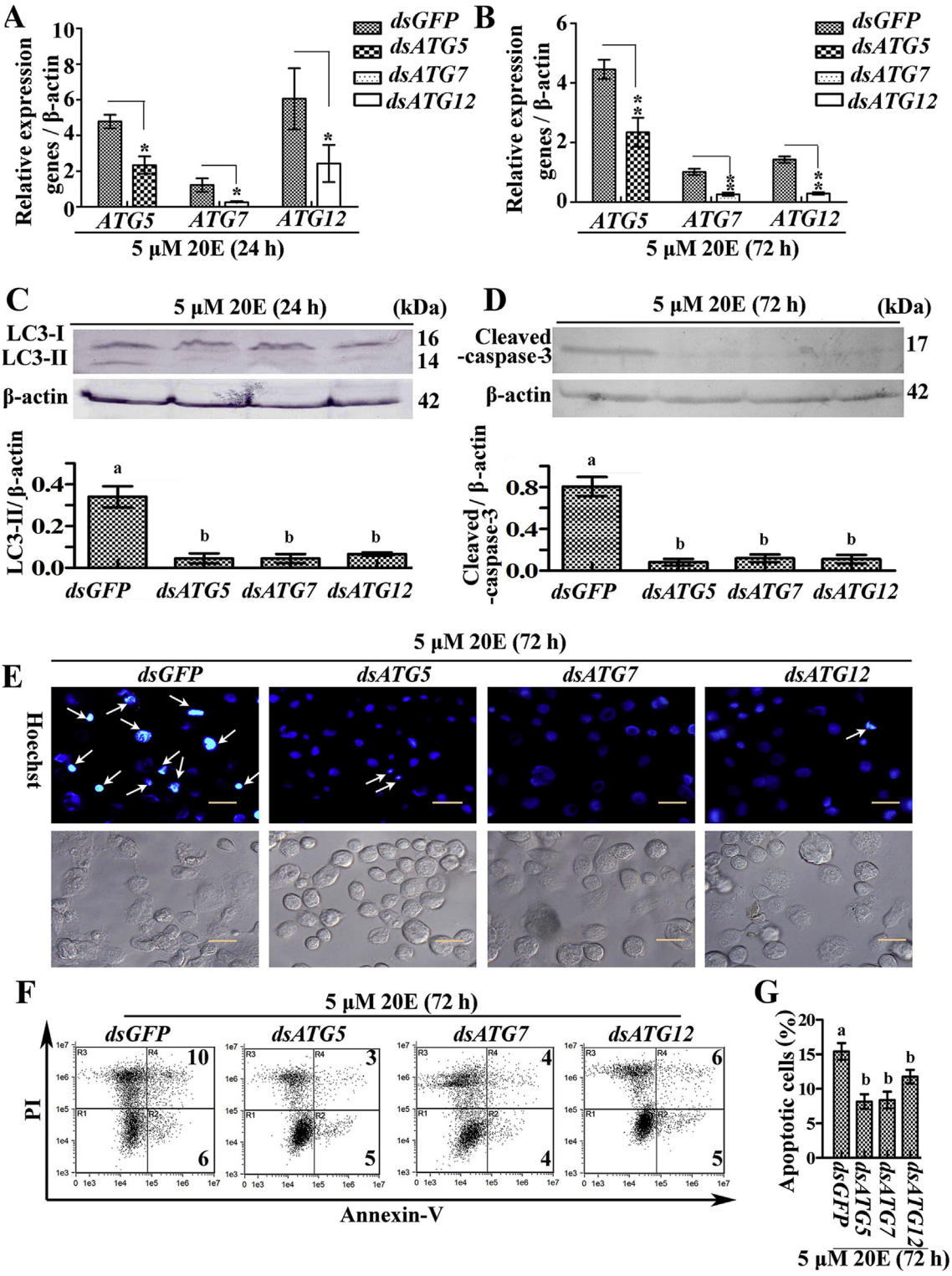

Fig. 5. Knockdown of *ATG5*, *7*, *12* repressed autophagy and apoptosis. **(A)** and **(B)** Statistical analysis of the effect of *ATG5*, *7* or *12* knockdown by qRT-PCR assay respectively, (20E 5 μM for 24 h or 72 h). β-actin was used as internal reference and the relative expression was checked with $2^{-\Delta\Delta T}$ method. *dsGFP* (500 ng for 48 h) as the negative control of *dsATG5*, *7*, *12* and *dsATG5*, *7 12* (500 ng for 48 h). DMSO as the solvent control of 20E. **(C)** Statistical analysis of LC3-II based on a Western blot assay. β-actin as the loading control and other treatments were same with A. **(D)** Statistical analysis of the level of Cleaved-caspase-3 based on a Western blot assay and other treatments were same with B except 20E (5 μM for 72 h). **(E)** Hoechst means Hoechst 33342 (Beyotime Biotechnology 10 μg/mL). Arrows showed the nucleus of apoptotic cells and other treatments were same with B. **(F)** Flow cytometry analysis of Annexin-V and propidium iodide (PI) staining after the same treatments with B. R1, normal cells; R2, early apoptotic cells; R3, died cells; R4, meddle and late apoptotic cells. The number in the picture means the percentage of apoptotic cells. **(G)** Statistic analysis of F. All of the experiments were performed in triplicate, and statistical analysis was conducted using Student's *t*-test (*$p < 0.05$ **$p < 0.01$), ANOVA. Bars represented the mean ± S. D, and different lowercase letters indicated significant differences ($p < 0.05$). The yellow bars represented 20 μm. (For interpretation of the references to colour in this figure legend, the reader is referred to the web version of this article.)

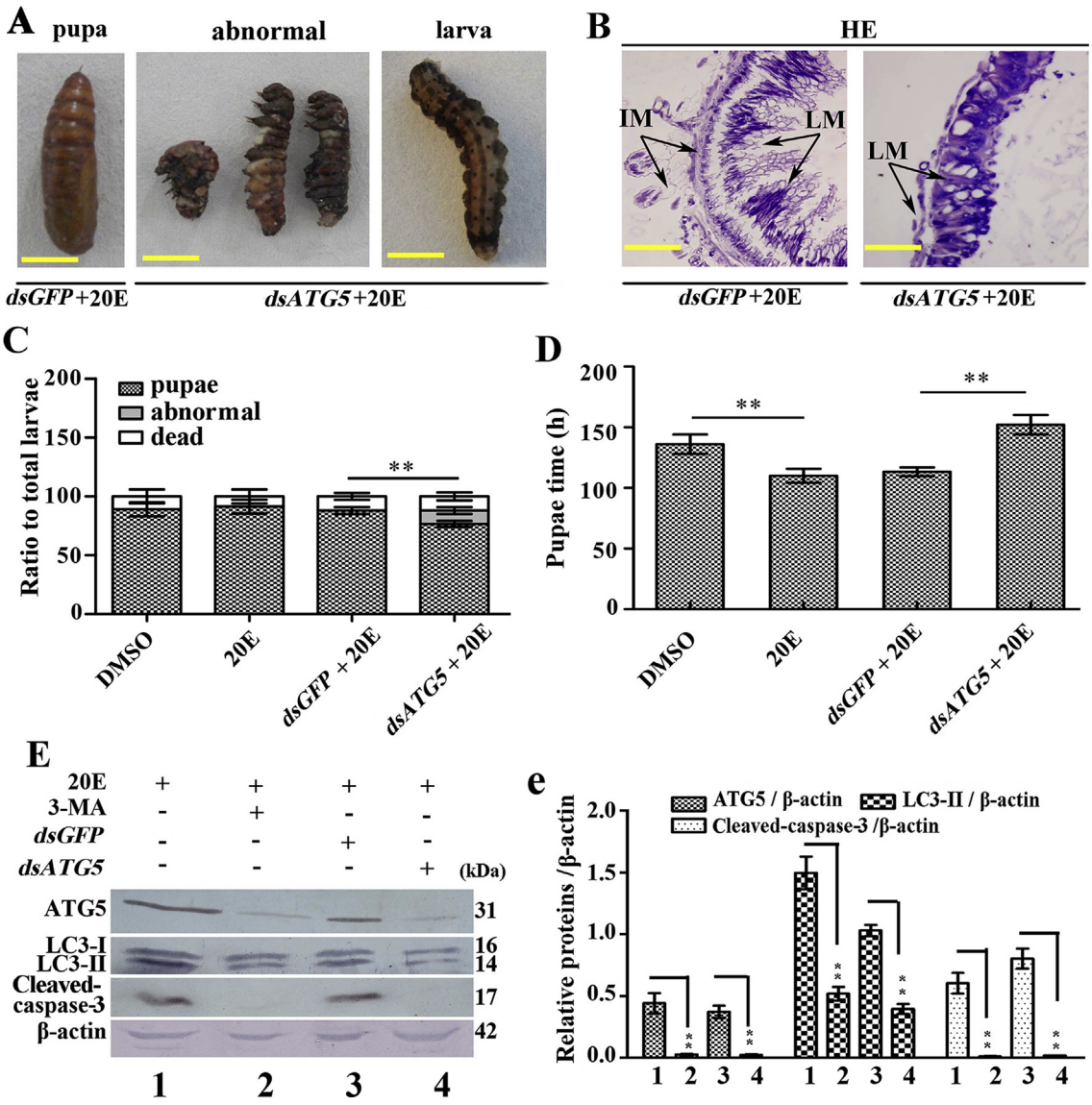

Fig. 6. Knockdown of *ATG5* in larvae blocked autophagy, apoptosis and midgut PCD. (A) Phenotype of pupae after knockdown of *ATG5* (dsRNA 500 ng per 6th instar 6 h larva, one time). The yellow bars represent 0.5 cm **(B)** HE–stained midgut after knockdown of *ATG5*, observed at 90 h after dsRNA injection. LM: larval midgut; IM: imaginal midgut. The yellow bars represented 10 μm. **(C)** Significance analysis of (A). **(D)** The significance analysis of the time that half larvae pupated. **(E)** Western blot assay for the expression of ATG5, LC3-I, LC3-II and Cleaved-caspase-3 after *ATG5* knockdown or injection of 3-MA (10 μM) in 6–96 h larvae. **(e)** Statistics and the significance analysis of (D). All of the experiments were performed in triplicate, and statistical analysis was conducted using Student's *t*-test (*p < 0.05 **p < 0.01). Bars represented the mean ± S. D. (For interpretation of the references to colour in this figure legend, the reader is referred to the web version of this article.)

increase in the larval midgut during metamorphosis.

Increase in 20E-induced Ca^{2+} level was examined in HaEpi cells to verify the 20E induction of the Ca^{2+} level in larvae. Red fluorescence indicated that the calcium increased along with the 20E concentration increase from 1, 2, 5, and 10 μM in 24 h (Fig. 8C and c). These data confirm that 20E induces calcium increase in the cells in a dose-dependent manner.

4. Discussion

Understanding how cells regulate the transformation of autophagy to apoptosis is critical for understanding the mechanisms of cell survival and death. Our studies in the lepidopteran insect *H. armigera* suggest that a steroid hormone, which is known as 20E, induces both autophagy and apoptosis during midgut PCD, with a lower concentration of 20E to induce autophagy and a higher concentration of 20E to induce the transformation of autophagy to apoptosis. Ca^{2+} is the key factor in determining the transformation of 20E-induced autophagy to apoptosis.

4.1. 20E induction of transformation of autophagy to apoptosis depends on the concentration

The steroid hormone 20E promotes autophagy and apoptosis in the fat body and midgut of *Bombyx* (Tian et al., 2013; Xie et al., 2016) as well as the midgut of *Drosophila* (Santhanam et al., 2014). This study indicates that 20E induces autophagy or apoptosis in a concentration-dependent manner. At low concentrations (1 μM), 20E had no obvious effect on the cells, whereas increased concentrations of 20E (2–5 μM) induced autophagy in 24 h. Higher concentrations of 20E (5–10 μM) induced apoptosis in 24 h. Therefore, the 20E concentration is a key factor in the transformation from autophagy to apoptosis in midgut cells. The titer of 20E is constantly changing during the development from larvae to

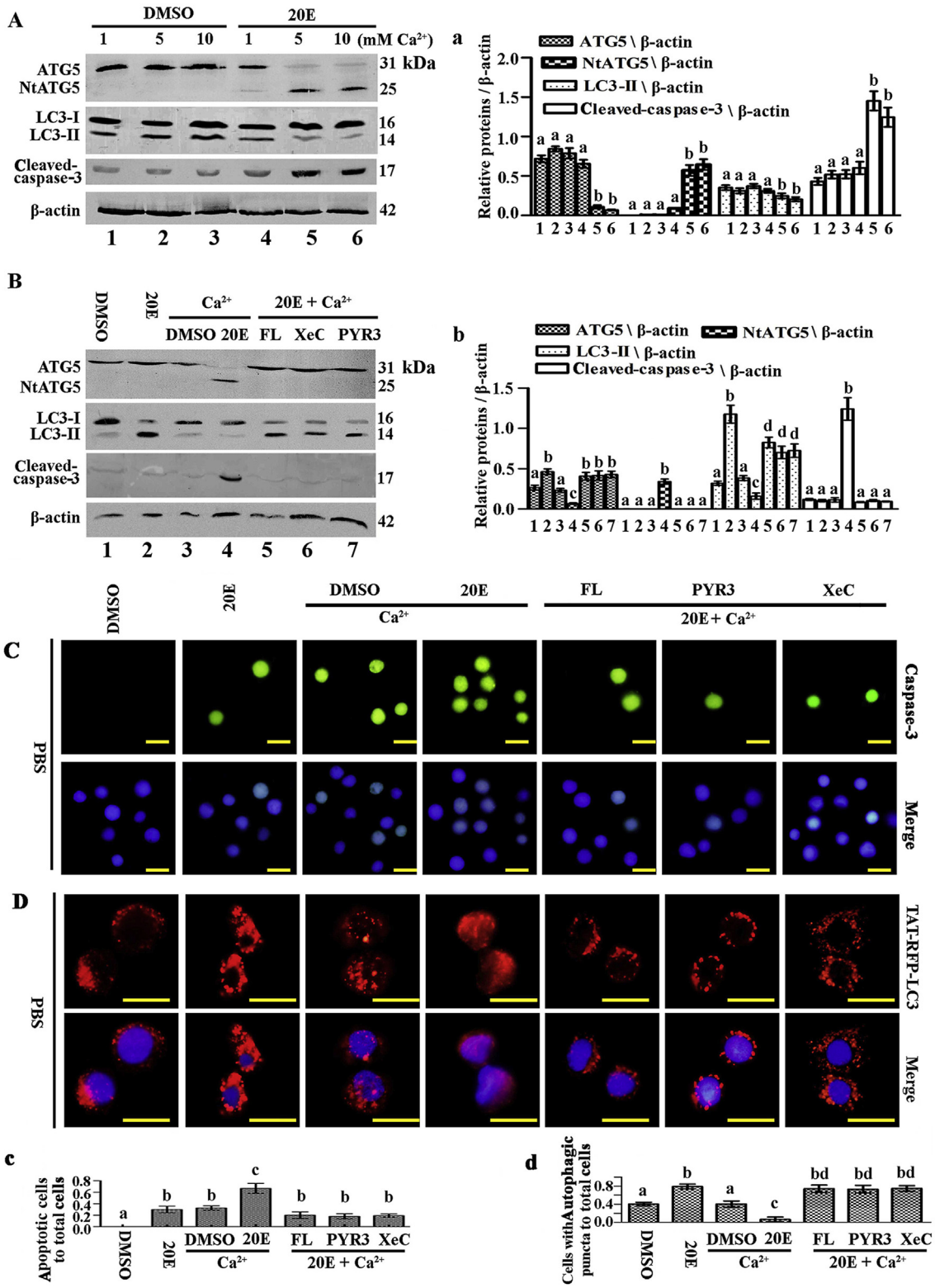

Fig. 7. Calcium regulated the 20E-induced formation of NtATG5, cleaved-caspase-3 and apoptosis. (A) Western blot assay for ATG5, NtATG5, LC3-I, LC3-II and Cleaved-caspase-3 levels at different Ca^{2+} concentrations in HaEpi cells induced by 20E (5 μM, 6 h) in PBS compared with DMSO. **(a)** Statistical analysis of (A). **(B)** Western blot assay to determine the expression of ATG5, NtATG5, LC3-I, LC3-II and Cleaved-caspase-3 after the indicated treatments. 20E (5 μM) for 6 h in PBS; Ca^{2+} (5 mM) in PBS for 2 min before 20E induction; and FL (5 μM), PYR3 (10 μM), and XeC (10 μM) for 30 min before 20E and Ca^{2+} induction. **(b)** Statistical analysis of (B). **(C)** Apoptosis detection using the NucView™ caspase-3 assay kit after the same treatments as in B. DAPI: staining nucleus blue. Merge: fusion of green and blue. **(c)** Statistical analysis of (C). **(D)** Addition of 2 μg of the TAT-RFP-LC3 protein in 2 mL of PBS to detect autophagy with the same treatments as in (B). **(d)** Statistical analysis of (D). DAPI: staining nucleus blue and merge: fusion of green and blue. All experiments were performed in triplicate, and statistical analysis was conducted using ANOVA. Bars represented the mean ± S. D, and different lowercase letters indicated significant differences ($p < 0.05$). The yellow bars represented 20 μm. (For interpretation of the references to colour in this figure legend, the reader is referred to the web version of this article.)

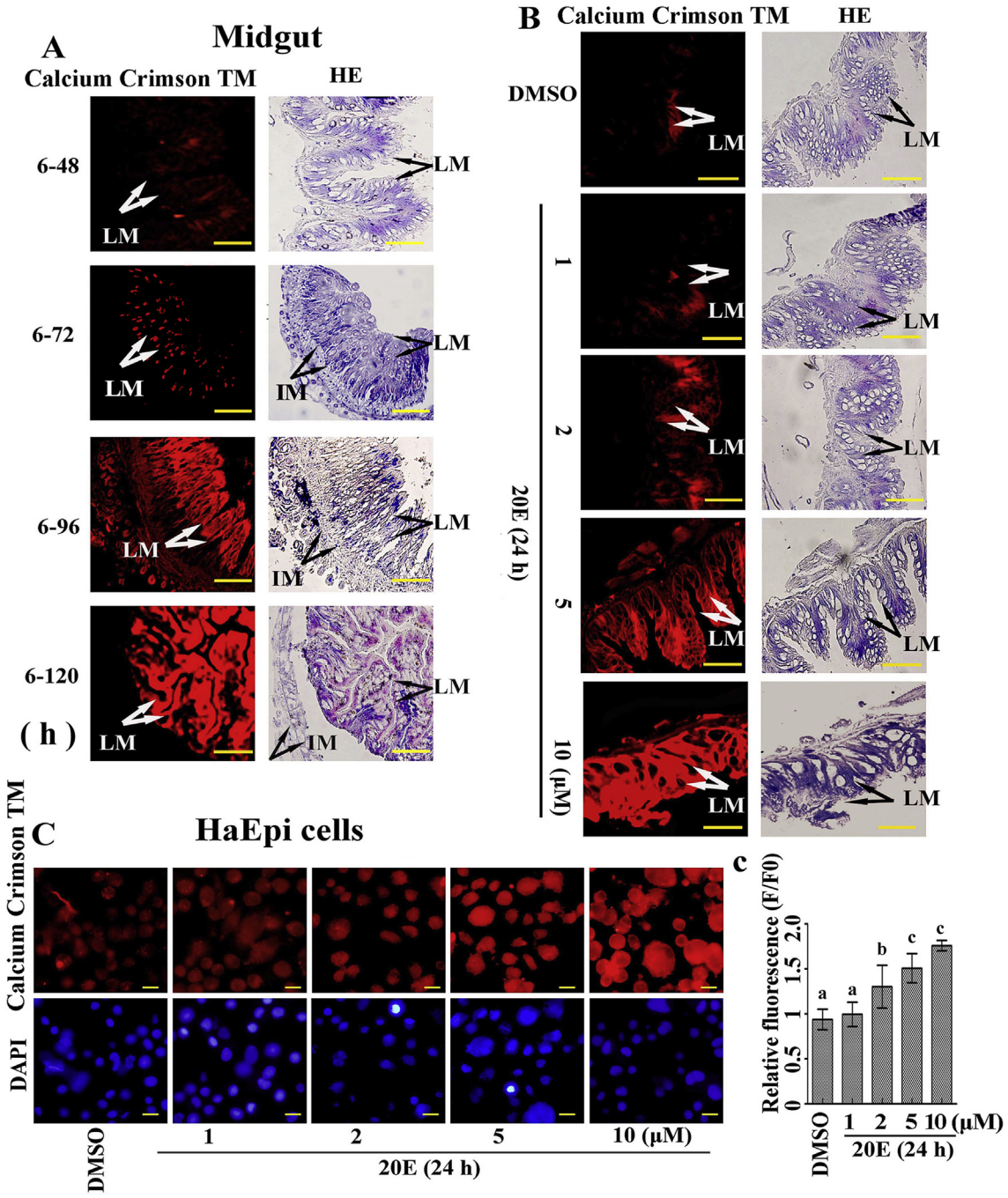

Fig. 8. 20E induced cellular Ca^{2+} increase. (A) The development hours of the sixth instar larvae were indicated by 6–48, 6–72, 6–96, and 6–120. IM represented imaginal midgut. LM represented larval midgut. The yellow bars represented 10 μm. Calcium Crimson™ dye was used to measure the Ca^{2+} concentration, and the strength of red fluorescence reflected the level of the Ca^{2+} concentration. HE staining showed the midgut morphology. **(B)** The 6-6 h larvae were injected with 20E (1, 2, 5, 10 μM) for 24 h and DMSO was used as the solvent control of 20E. The other graphical representation was the same with (A). **(C)** The HaEpi cells were treated with 20E (1, 2, 5, 10 μM) for 24 h in Grace's medium, and DMSO was used as the solvent control of 20E. **F**: average fluorescence signal of cells after 20E treatment, **F0**: average fluorescence after DMSO treatment for 24 h. **(c)** Statistical analysis of (C). All experiments were performed in triplicate, and statistical analysis was conducted using ANOVA. Bars represented the mean ± S. D, and different lowercase letters indicated significant differences ($p < 0.05$). The yellow bars represented 20 μm. (For interpretation of the references to colour in this figure legend, the reader is referred to the web version of this article.)

pupae. The 20E titer is 1 μM during feeding, reaching a maximum of approximately 4.2 μg/mL (8.6 μM) at the molt stage in lepidopteran *Manduca sexta* (Langelan et al., 2000).

4.2. 20E induces an intracellular Ca^{2+} increase to transform autophagy to apoptosis

Ca^{2+} plays an important role in cell proliferation, differentiation, and apoptosis (Liang and Lu, 2012; Rouzaire-Dubois et al., 2005). 20E induces intracellular Ca^{2+} by G-protein-coupled receptor (GPCR)-phospholipase C (PLC)-inositol-1,4,5-triphosphate (IP3) pathway in *B. mori* and *H. armigera* (Liu et al., 2014; Manaboon et al., 2009). In HaEpi cells, 20E-induced Ca^{2+} influx promotes apoptosis (Wang et al., 2016), and 20E-induced Ca^{2+} influx can be blocked by three inhibitors (FL, Pyr3, or Xec) (Liu et al., 2014). Therefore, all three inhibitors abolished 20E-induced apoptosis.

The Ca^{2+} concentration in Grace's medium was approximately 6–7 mM, and the cells in this study were incubated in PBS to exclude the effect of Ca^{2+} in the medium. Incubation in PBS for a long time induced apoptosis; however, within 6 h, apoptosis was not induced without 20E and Ca^{2+} induction. The increase in Ca^{2+} can activate protease calpain (Alexa et al., 2004); the activated-calpains can lead to unregulated proteolysis of both target and non-target proteins, resulting in irreversible tissue damage (Liu et al., 2008). The full-length ATG5 plays a role in autophagy (Shi et al., 2013). The cleavage of ATG5 depends on the activation of calpain, which cleaves ATG5 to produce NtATG5, thereby inducing the release of cytochrome *c* from mitochondrion to enhance apoptosis (Yousefi et al., 2006). In *B. mori* Bm-12 cells, knockdown of *ATG5* decreases the release of cytochrome *c* from the mitochondrion and the reduction of caspase-3 activity (Xie et al., 2016). In our previous study, the apoptosis inhibitor survivin prevents insect midgut from cell death during postembryonic development, thereby suggesting that IAPs are also involved in insect midgut PCD (He et al., 2012). Our study revealed that when calcium channels are blocked, ATG5 can not be cleaved to NtATG5, and autophagy was enhanced. With increased calcium levels, ATG5 was cleaved to NtATG5 and LC3-II and autophagosome vesicles disappeared. The cleaved-caspase-3 level increased to induce apoptotic cell death. The increase of the cellular Ca^{2+} concentration depended on the 20E concentration and induction time. The cellular Ca^{2+} concentration gradually increased with the increase in 20E concentration. Thus, we can conclude that a high concentration of 20E induced a high cellular Ca^{2+} level to transform autophagy to apoptosis.

4.3. Autophagy proteins are necessary for apoptosis in 20E-mediated midgut PCD

Both autophagy and apoptosis are observed in insect midgut PCD. Autophagic cell death is observed in *Drosophila* midgut (Denton et al., 2009). Autophagy precedes apoptosis in *Bombyx* midgut (Franzetti et al., 2012). In the *H. armigera* midgut, knockdown of *ATG5* inhibited both autophagy and apoptosis, which delayed the midgut PCD and pupation time. In the experiments, 20E was injected followed by *ATG5* knockdown. Therefore, ATG5 is necessary for autophagy, apoptosis, and final pupation. In mammals, the release of cytochrome *c* from mitochondria to cytosol enhances apoptosis by activating the initiator caspases and effector caspases (Maiuri et al., 2007). In *Drosophila*, cytochrome *c* does not play any role in apoptosis (Hay and Guo, 2006). However, in *Lepidopteran* insects such as *Spodoptera frugiperda* Sf21 cells (Jin et al., 2012) and *Bombyx* Bm-12 cells (Xie et al., 2016), apoptosis depends on cytochrome *c* release. *ATG5* interference decreased ATG5 in our study, thereby decreasing NtATG5. The involvement of mitochondrial cytochrome c in the apoptosis should be examined in the future work.

Our HaEpi cell study shows that when autophagy is inhibited by 3-MA or interfered with the key autophagy genes *ATG5*, *ATG7*, or *ATG12*, autophagic vesicles and LC3-II decrease and cleaved-caspase-3 drastically decreases, thereby indicating that autophagy proteins are necessary for both autophagy and apoptosis. In contrast, inhibition of caspase-3 activity by the caspase-3 inhibitor Ac-DEVD-CHO has little effect on LC3-II and autophagic vesicle formation, thereby indicating that the suppression of apoptosis could maintain autophagy and cell survival.

5. Conclusion

20E induces autophagy at a low concentration or short treatment duration. However, at high concentrations or long treatment periods, 20E transforms autophagy to apoptosis. Higher concentrations of 20E mediates an intracellular Ca^{2+} increase to regulate the cleavage of ATG5 to NtATG5 and caspase-3 to active caspase-3 for apoptotic cell death. Blocking Ca^{2+} channels represses apoptosis and maintains autophagy and cell survival. 20E simultaneously triggers autophagy and intracellular Ca^{2+} increase, thereby resulting in midgut PCD by autophagy to apoptosis transformation (Fig. 9).

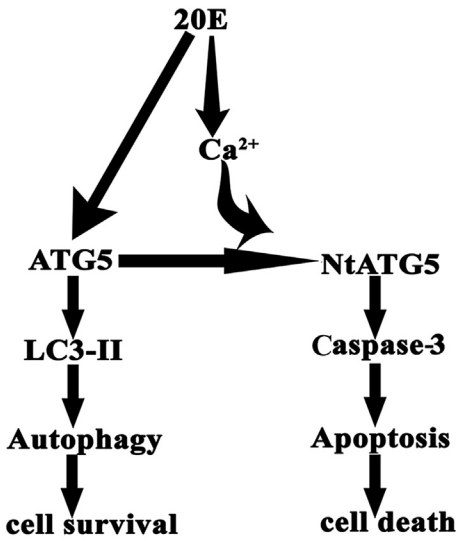

Fig. 9. Explanation of higher intracellular calcium levels switching autophagy to apoptosis by 20E induction. 20E promotes the increase of LC3-II through ATG5 and then induces autophagy, leading to cell survival. The intracellular Ca^{2+} level gradually increases as the 20E concentration elevation, which results in the cleavage of ATG5 to NtATG5, activation of caspase-3, and tendency of cells toward apoptotic cell death. Therefore, higher intracellular calcium switches autophagy to apoptosis under 20E induction.

Conflict of interest

The authors declare that they have no conflicts of interest with the contents of this article.

Author contributions

YB Li performed and analyzed the experiments. T Yang and XR Li prepared the antibodies against *H. armigera* LC3. JX Wang and XF Zhao conceived and coordinated the study and edited the paper. All authors reviewed the results and approved the final version of the manuscript. ALL co-authors have checked and confirmed their contribution statement.

Acknowledgments

This study was supported by grants from the National Natural Science Foundation of China (31230067 and 31572328).

References

Alexa, A., Bozoky, Z., Farkas, A., Tompa, P., Friedrich, P., 2004. Contribution of distinct structural elements to activation of calpain by Ca^{2+} ions. J. Biol. Chem. 279, 20118–20126.
Baehrecke, E.H., 2005. Autophagy: dual roles in life and death? Nature reviews. Mol. Cell Biol. 6, 505–510.
Berridge, M.J., Lipp, P., Bootman, M.D., 2000. The versatility and universality of calcium signalling. Nat. Rev. Mol. Cell Biol. 1, 11–21.
Berry, D.L., Baehrecke, E.H., 2007. Growth arrest and autophagy are required for salivary gland cell degradation in *Drosophila*. Cell 131, 1137–1148.
Bhutia, S.K., Das, S.K., Azab, B., Dash, R., Su, Z.Z., Lee, S.G., Dent, P., Curiel, D.T.,

Sarkar, D., Fisher, P.B., 2011. Autophagy switches to apoptosis in prostate cancer cells infected with melanoma differentiation associated gene-7/interleukin-24 (mda-7/IL-24). Autophagy 7, 1076–1077.
Bradford, M.M., 1976. A rapid and sensitive method for the quantitation of microgram quantities of protein utilizing the principle of protein-dye binding. Anal. Biochem. 72, 248–254.
Burman, C., Ktistakis, N.T., 2010. Regulation of autophagy by phosphatidylinositol 3-phosphate. FEBS Lett. 584, 1302–1312.
Cai, M.J., Dong, D.J., Wang, Y., Liu, P.C., Liu, W., Wang, J.X., Zhao, X.F., 2014. G-protein-coupled receptor participates in 20-hydroxyecdysone signaling on the plasma membrane. Cell Commun. Signal. CCS 12, 9.
Clapham, D.E., 2007. Calcium signaling. Cell 131, 1047–1058.
Courtiade, J., Pauchet, Y., Vogel, H., Heckel, D.G., 2011. A comprehensive characterization of the caspase gene family in insects from the order *Lepidoptera*. BMC genomics 12, 357.
De Smet, P., Parys, J.B., Callewaert, G., Weidema, A.F., Hill, E., De Smedt, H., Erneux, C., Sorrentino, V., Missiaen, L., 1999. Xestospongin C is an equally potent inhibitor of the inositol 1,4,5-trisphosphate receptor and the endoplasmic-reticulum Ca(2+) pumps. Cell calcium 26, 9–13.
Denton, D., Shravage, B., Simin, R., Mills, K., Berry, D.L., Baehrecke, E.H., Kumar, S., 2009. Autophagy, not apoptosis, is essential for midgut cell death in *Drosophila*. Curr. Biol. CB 19, 1741–1746.
Fang, L., Li, X., Luo, Y., He, W., Dai, C., Yang, J., 2014. Autophagy inhibition induces podocyte apoptosis by activating the pro-apoptotic pathway of endoplasmic reticulum stress. Exp. Cell Res. 322, 290–301.
Franzetti, E., Huang, Z.J., Shi, Y.X., Xie, K., Deng, X.J., Li, J.P., Li, Q.R., Yang, W.Y., Zeng, W.N., Casartelli, M., Deng, H.M., Cappellozza, S., Grimaldi, A., Xia, Q., Feng, Q., Cao, Y., Tettamanti, G., 2012. Autophagy precedes apoptosis during the remodeling of silkworm larval midgut. Apoptosis Int. J. Program. Cell death 17, 305–324.
Friedrich, P., 2004. The intriguing Ca^{2+} requirement of calpain activation. Biochem. biophysical Res. Commun. 323, 1131–1133.
Hakim, R.S., Baldwin, K., Smagghe, G., 2010. Regulation of midgut growth, development, and metamorphosis. Annu. Rev. entomology 55, 593–608.
Hay, B.A., Guo, M., 2006. Caspase-dependent cell death in *Drosophila*. Annu. Rev. Cell Dev. Biol. 22, 623–650.
He, H.J., Hou, L., Wang, J.X., Zhao, X.F., 2012. The apoptosis inhibitor survivin prevents insect midgut from cell death during postembryonic development. Mol. Biol. Rep. 39, 1691–1699.
Herrero-Martin, G., Hoyer-Hansen, M., Garcia-Garcia, C., Fumarola, C., Farkas, T., Lopez-Rivas, A., Jaattela, M., 2009. TAK1 activates AMPK-dependent cytoprotective autophagy in TRAIL-treated epithelial cells. EMBO J. 28, 677–685.
Hoyer-Hansen, M., Bastholm, L., Szyniarowski, P., Campanella, M., Szabadkai, G., Farkas, T., Bianchi, K., Fehrenbacher, N., Elling, F., Rizzuto, R., Mathiasen, I.S., Jaattela, M., 2007. Control of macroautophagy by calcium, calmodulin-dependent kinase kinase-beta, and Bcl-2. Mol. Cell 25, 193–205.
Iga, M., Manaboon, M., Matsui, H., Sakurai, S., 2010. Ca^{2+}-PKC-caspase 3-like protease pathway mediates DNA and nuclear fragmentation in ecdysteroid-induced programmed cell death. Mol. Cell Endocrinol. 321, 146–151.
Jin, C., Wu, S., Lu, X., Liu, Q., Zhang, L., Yang, J., Xi, Q., Cai, Y., 2012. Conditioned medium from actinomycin D-treated apoptotic cells induces mitochondria-dependent apoptosis in bystander cells. Toxicol. Lett. 211, 45–53.
Kiyonaka, S., Kato, K., Nishida, M., Mio, K., Numaga, T., Sawaguchi, Y., Yoshida, T., Wakamori, M., Mori, E., Numata, T., Ishii, M., Takemoto, H., Ojida, A., Watanabe, K., Uemura, A., Kurose, H., Morii, T., Kobayashi, T., Sato, Y., Sato, C., Hamachi, I., Mori, Y., 2009. Selective and direct inhibition of TRPC3 channels underlies biological activities of a pyrazole compound. Proc. Natl. Acad. Sci. U. S. A. 106, 5400–5405.
Langelan, R.E., Fisher, J.E., Hiruma, K., Palli, S.R., Riddiford, L.M., 2000. Patterns of MHR3 expression in the epidermis during a larval molt of the tobacco hornworm *Manduca sexta*. Dev. Biol. 227, 481–494.
Liang, C., 2010. Negative regulation of autophagy. Cell death Differ. 17, 1807–1815.
Liang, W.Z., Lu, C.H., 2012. Carvacrol-induced [Ca2+]i rise and apoptosis in human glioblastoma cells. Life Sci. 90, 703–711.
Liu, J., Liu, M.C., Wang, K.K., 2008. Calpain in the CNS: from synaptic function to neurotoxicity. Sci. Signal. 1 re1.
Liu, M., Udhe-Stone, C., Goudar, C.T., 2011. Progress curve analysis of qRT-PCR reactions using the logistic growth equation. Biotechnol. Prog. 27, 1407–1414.
Liu, P., Peng, H.J., Zhu, J., 2015. Juvenile hormone-activated phospholipase C pathway enhances transcriptional activation by the methoprene-tolerant protein. Proc. Natl. Acad. Sci. U. S. A. 112, E1871–E1879.
Liu, W., Cai, M.J., Zheng, C.C., Wang, J.X., Zhao, X.F., 2014. Phospholipase C gamma 1 connects the cell membrane pathway to the nuclear receptor pathway in insect steroid hormone signaling. J. Biol. Chem. 289, 13026–13041.
Maiuri, M.C., Zalckvar, E., Kimchi, A., Kroemer, G., 2007. Self-eating and self-killing: crosstalk between autophagy and apoptosis. Nature reviews. Mol. Cell Biol. 8, 741–752.
Manaboon, M., Iga, M., Iwami, M., Sakurai, S., 2009. Intracellular mobilization of Ca^{2+} by the insect steroid hormone 20-hydroxyecdysone during programmed cell death in silkworm anterior silk glands. J. insect physiology 55, 122–128.
Pinter, M., Friedrich, P., 1988. The calcium-dependent proteolytic system calpain-calpastatin in *Drosophila melanogaster*. Biochem. J. 253, 467–473.
Pyo, J.O., Jang, M.H., Kwon, Y.K., Lee, H.J., Jun, J.I., Woo, H.N., Cho, D.H., Choi, B., Lee, H., Kim, J.H., Mizushima, N., Oshumi, Y., Jung, Y.K., 2005. Essential roles of Atg5 and FADD in autophagic cell death: dissection of autophagic cell death into vacuole formation and cell death. J. Biol. Chem. 280, 20722–20729.
Rabinowitz, J.D., White, E., 2010. Autophagy and metabolism. Science 330, 1344–1348.
Romanelli, D., Casati, B., Franzetti, E., Tettamanti, G., 2014. A molecular view of autophagy in *Lepidoptera*. Biomed. Res. Int. 2014, 902315.
Rouzaire-Dubois, B., O'Regan, S., Dubois, J.M., 2005. Cell size-dependent and independent proliferation of rodent neuroblastoma x glioma cells. J. Cell. physiology 203, 243–250.
Santhanam, A., Peng, W.H., Yu, Y.T., Sang, T.K., Chen, G.C., Meng, T.C., 2014. Ecdysone-induced receptor tyrosine phosphatase PTP52F regulates *Drosophila* midgut histolysis by enhancement of autophagy and apoptosis. Mol. Cell. Biol. 34, 1594–1606.
Shao, H.L., Zheng, W.W., Liu, P.C., Wang, Q., Wang, J.X., Zhao, X.F., 2008. Establishment of a new cell line from lepidopteran epidermis and hormonal regulation on the genes. PloS one 3, e3127.
Shi, M., Zhang, T., Sun, L., Luo, Y., Liu, D.H., Xie, S.T., Song, X.Y., Wang, G.F., Chen, X.L., Zhou, B.C., Zhang, Y.Z., 2013. Calpain, Atg5 and Bak play important roles in the crosstalk between apoptosis and autophagy induced by influx of extracellular calcium. Apoptosis Int. J. Program. Cell death 18, 435–451.
Sui, Y.P., Wang, J.X., Zhao, X.F., 2009. The impacts of classical insect hormones on the expression profiles of a new digestive trypsin-like protease (TLP) from the cotton bollworm, *Helicoverpa armigera*. Insect Mol. Biol. 18, 443–452.
Tasdemir, E., Galluzzi, L., Maiuri, M.C., Criollo, A., Vitale, I., Hangen, E., Modjtahedi, N., Kroemer, G., 2008. Methods for assessing autophagy and autophagic cell death. Methods Mol. Biol. 445, 29–76.
Terland, O., Flatmark, T., 1999. Drug-induced parkinsonism: cinnarizine and flunarizine are potent uncouplers of the vacuolar H+-ATPase in catecholamine storage vesicles. Neuropharmacology 38, 879–882.
Tettamanti, G., Grimaldi, A., Pennacchio, F., de Eguileor, M., 2007. *Lepidopteran* larval midgut during prepupal instar: digestion or self-digestion? Autophagy 3, 630–631.
Tian, L., Ma, L., Guo, E., Deng, X., Ma, S., Xia, Q., Cao, Y., Li, S., 2013. 20-Hydroxyecdysone upregulates Atg genes to induce autophagy in the *Bombyx* fat body. Autophagy 9, 1172–1187.
Torkzadeh-Mahani, M., Ataei, F., Nikkhah, M., Hosseinkhani, S., 2012. Design and development of a whole-cell luminescent biosensor for detection of early-stage of apoptosis. Biosens. Bioelectron. 38, 362–368.
Tracy, K., Baehrecke, E.H., 2013. The role of autophagy in *Drosophila* metamorphosis. Curr. Top. Dev. Biol. 103, 101–125.
Wang, C.L., Xia, Y., Nie, J.Z., Zhou, M., Zhang, R.P., Niu, L.L., Hou, L.H., Cao, X.H., 2013. *Musca domestica* larva lectin induces apoptosis in BEL-7402 cells through a Ca(2+)/JNK-mediated mitochondrial pathway. Cell Biochem. biophysics 66, 319–329.
Wang, D., Pei, X.Y., Zhao, W.L., Zhao, X.F., 2016. Steroid hormone 20-hydroxyecdysone promotes higher calcium mobilization to induce apoptosis. Cell Calcium 60, 1–12.
Xie, K., Tian, L., Guo, X., Li, K., Li, J., Deng, X., Li, Q., Xia, Q., Zhong, Y., Huang, Z., Liu, J., Li, S., Yang, W., Cao, Y., 2016. BmATG5 and BmATG6 mediate apoptosis following autophagy induced by 20-hydroxyecdysone or starvation. Autophagy 11, 381–396.
Yousefi, S., Perozzo, R., Schmid, I., Ziemiecki, A., Schaffner, T., Scapozza, L., Brunner, T., Simon, H.U., 2006. Calpain-mediated cleavage of Atg5 switches autophagy to apoptosis. Nat. Cell Biol. 8, 1124–1132.
Yu, L., Alva, A., Su, H., Dutt, P., Freundt, E., Welsh, S., Baehrecke, E.H., Lenardo, M.J., 2004. Regulation of an ATG7-beclin 1 program of autophagic cell death by caspase-8. Science 304, 1500–1502.
Zhao, W.L., Wang, D., Liu, C.Y., Zhao, X.F., 2016. G-protein-coupled receptor kinase 2 terminates G-protein-coupled receptor function in steroid hormone 20-hydroxyecdysone signaling. Sci. Rep. 6, 29205.
Zhou, Z., Li, Y., Yuan, C., Zhang, Y., Qu, L., 2015. Oral administration of TAT-PTD-Diapause hormone fusion protein interferes with *Helicoverpa armigera* (Lepidoptera: Noctuidae) development. J. insect Sci. 15.
Zocchi, M.R., Rubartelli, A., Morgavi, P., Poggi, A., 1998. HIV-1 Tat inhibits human natural killer cell function by blocking L-type calcium channels. J. Immunol. 161, 2938–2943.